A Review on Utilizing Modern Technologies to Enhance the Seismic Resistance of Ancient Wooden Structures

Siqi Shen
DUNDEE INTERNATIONAL INSTITUTE OF CENTRAL SOUTH UNIVERSITY, CENTRAL SOUTH UNIVERSITY, CHANGSHA, HUNAN,410083, China
2013745238@QQ.COM

Abstract

Ancient wooden structures, as crucial carriers of historical and cultural heritage, exhibit significantly reduced seismic resistance due to the degradation of material mechanical properties caused by long-term environmental erosion. Under strong earthquakes, they are highly susceptible to characteristic seismic damage such as bracket set dislocation, column frame tilting, and roof collapse. Systematically investigating their seismic mechanisms and innovating energy dissipation technologies and structural reinforcement methods compatible with heritage conservation principles are essential for enhancing their seismic resilience and sustainable preservation capability. This review summarizes the principles and limitations of the triple seismic mitigation mechanisms—"sliding isolation - joint energy dissipation - mass tuning"—formed through the synergistic effects of column-base slippage, rotation of semi-rigid mortise-tenon joints, energy dissipation within dougong brackets, and roof inertial forces in ancient wooden structures. It focuses on the primary technical approaches currently employed both domestically and internationally to enhance seismic performance: joint reinforcement techniques, which improve load-bearing capacity and stiffness using steel components, fiber-reinforced composites, screws, or wooden wedges; energy dissipation technologies, which introduce devices like friction dampers, shape memory alloy dampers, viscoelastic dampers, and isolation systems to dissipate seismic energy; and column base hooping techniques aimed at optimizing the column rocking mechanism. Research indicates that while modern reinforcement techniques effectively improve structural safety, they commonly increase structural stiffness, amplify seismic actions, adversely affect internal force redistribution, and compromise architectural historic authenticity. Future research should prioritize developing bio-sourced materials or traditional craft-compatible devices that ensure sufficient damping while adhering to the authenticity principle of heritage conservation.

Keywords：structure; seismic; mechanism; energy

1. Research Background and Significance of the Topic Selection

1.1 Research background and significance of the topic selection

Timber structural heritage buildings, as historical crystallizations of human material and spiritual civilization, profoundly embody the aesthetic paradigms and engineering ingenuity of their respective eras. Serving as vital physical vessels for cultural and historical transmission, they possess irreplaceable historical, cultural, and scientific significance. Subjected to centuries of environmental degradation—including but not limited to wind erosion, rain infiltration, biological decay, and cyclic hygrothermal effects—the mechanical properties of timber materials exhibit significant deterioration. Key structural components, particularly mortise-tenon joints, experience reduced constraint efficiency due to loosening, leading to pronounced time-dependent degradation in the overall structural system's load-bearing capacity. Under intense seismic actions, such structures are highly susceptible to accumulating inelastic deformations owing to stiffness degradation, insufficient damping mechanisms, and limited hysteretic energy dissipation capacity. This vulnerability may consequently trigger characteristic seismic damage patterns such as bracket set dislocation, column frame tilting, and roof collapse, potentially resulting in irreversible cultural heritage loss.

Therefore, systematically investigating the seismic mechanisms of ancient timber structures, and innovating energy dissipation technologies and structural reinforcement methods compatible with heritage conservation principles, are critically significant for enhancing their seismic resilience and sustainable preservation capability. This endeavor represents not only a frontier research topic in structural engineering but also constitutes a scientific imperative within the field of cultural heritage conservation.

2. The Seismic Resistance Principles and Improvements of Ancient Wooden Architecture

2.1 The architectural structure of ancient wooden buildings

Ancient timber structures achieve seismic resilience through a unique structural system: Pinned column-base connections form friction-sliding isolation interfaces; semi-rigid mortise-tenon joints generate hysteretic energy dissipation; dou-gong brackets act as kinetic energy transmission hubs that dissipate seismic forces through compression-reset mechanisms; while the massive roof utilizes mass concentration effects to provide inertial self-centering forces. These four components synergistically create a triple seismic mitigation mechanism integrating "sliding isolation - joint energy dissipation - mass tuning (Wang Long et al., 2024) [1].

2.2 Structural seismic resistance principles and limitations

2.2.1 Column-base

Seismic Resistance Principles: The floating column-base connection system formed by timber columns and plinths provides initial lateral stiffness through interfacial friction effects under low-intensity earthquakes. When horizontal seismic actions exceed the Coulomb friction threshold, controlled slippage occurs at the column-based interface. This mechanism dissipates seismic energy through friction work conversion while prolonging the natural vibration period. Essentially constituting a passive isolation system, it significantly reduces acceleration responses in the superstructure (Wang Long et al., 2024) [1].

Limitations: When the slippage at the column-based interface remains within critical thresholds, the structure maintains its vertical load-bearing capacity. However, excessive slippage that induces geometric eccentricity exceeding allowable limits (typically >0.25D, where D denotes column diameter) generates significant additional bending moments. This leads to compressive buckling instability of wood fibers, ultimately triggering progressive collapse of local load-bearing systems (Wang Long et al., 2024) [1].

2.2.2 Mortise-tenon Joints

Seismic Resistance Principles: Mortise-tenon joints serve as fundamental connecting units in ancient timber structures, extending from localized Dougong components to global beam-column systems (Li Jiaxu et al., 2021). Failure at these critical junctures may trigger progressive structural collapse. Wooden columns and beams are connected via mortise-tenon joints, forming a semi-rigid structural system. This system possesses a certain bending resistance while simultaneously accommodating significant torsional deformation. This characteristic results in the tenon and mortise primarily being subjected to compressive forces. When external forces, such as seismic activity, act upon the structure, deformation occurs at the joint interface due to mutual friction and compression between the tenon and mortise. This process effectively dissipates the seismic input energy, achieving the effects of energy dissipation and seismic reduction (Wang Long et al., 2024) [1].

Limitations: Phenomena such as tenon withdrawal, tenon fracture, and joint disengagement are characterized by the failure of mortise-tenon joints, leading to relative slippage or complete separation between structural members. Such damage will inevitably lead to structural tilting and even overall collapse (Wang Long et al., 2024) [1].

2.2.3 Dou-gong brackets

Seismic Resistance Principles: The Dougong system utilizes the base block as its foundation, with components such as bracket arms (Dou), bow-shaped brackets (Gong), lever arms, and beams progressively layered atop it. These elements interlock via nested mortise joints, forming a variable-stiffness structural system. Under seismic loading, compressive deformation between components effectively dissipates energy. Simultaneously, hidden connectors within the system undergo plastic deformation during earthquakes, establishing a secondary energy dissipation mechanism (Wang Long et al., 2024) [1].

Limitations: Under strong seismic actions, Dougong components are prone to splitting failure, crushing instability, and potential dislodgment. Concurrently, due to insufficient shear capacity, hidden connectors exhibit high susceptibility to shear fracture, resulting in joint connection failure (Wang Long et al., 2024) [1].

2.2.4 Roof

Seismic Resistance Principles: The dead load effects from the roof structure's self-weight enhance the tightness of mortise-tenon joints while improving the anti-sliding performance at contact surfaces between Dougong systems and column bases, thereby sustaining the overall structural stability (Wang Long et al., 2024) [1].

Limitations: Excessive self-weight of the roof structure significantly amplifies seismic inertial forces. Simultaneously, structurally deficient connections of roof attachments such as tiles and ridge ornaments present a dislodgment hazard under strong seismic actions (Wang Long et al., 2024) [1].

2.3 Methods for enhancing seismic resistance

2.3.1 Joint Reinforcement

Joint reinforcement techniques can substantially enhance structural load-bearing capacity, with typical methods including steel member reinforcement, fiber-reinforced composite strengthening, and screw reinforcement. However, these interventions generally increase structural stiffness, consequently amplifying seismic forces acting on the entire structure. Furthermore, inadequate consideration of internal force redistribution mechanisms may lead to adverse effects such as stress concentration and imbalanced nodal force redistribution when implementing localized over-reinforcement (Wang Long et al., 2024) [1].

2.3.2 Energy dissipation

Energy dissipation technology protects primary structures by redirecting seismic energy to supplemental devices, reducing the inelastic deformation demand on structural members. Key advantages include substantially increased structural damping ratios and efficient seismic energy absorption through device plastic deformation, all without modifying the mechanical properties of original components. Representative devices encompass elastomeric dampers, friction dampers, and shape memory alloy systems (Wang Long et al., 2024) [1].

2.3.3 Column Base Hooping

The column base hooping technique optimizes the timber column's rocking mechanism by enlarging the bearing area, significantly enhancing structural restoring force characteristics and overturning resistance stability. Simultaneously, it improves energy dissipation performance and progressive collapse resistance at the column-foot joints (Wang Long et al., 2024) [1].

3. Current research status both at home and abroad

3.1 Joint reinforcement

3.1.1 Joint damage mechanism

Li Jiaxu et al. [2] conducted seismic damage analyses on three sets of penetrating mortise-tenon joints based on the Diao Bo seismic damage model, Kratzig seismic damage model, and a modified Kratzig seismic damage model, establishing correlations between damage index and seismic fortification levels. The research results are shown in Table 2.

Table 1 Correlation between Damage Index and Seismic Fortification Levels [2]

Seismic Fortification Objective	*Damage Stage*	*Damage Grade*	*D*	*Damage Phenomena*
No damage under minor earthquakes	Damage initiation stage	Essentially intact	0~0.2	Penetrating tenon joints tightened, virtually undamaged
Repairable under moderate earthquakes	Damage development stage	Slight damage	0.2~0.4	Initial tenon withdrawal (<1cm), compressive deformation observed
	Moderate damage stage	Moderate damage	0.4~0.6	Tenon withdrawal (1~1.5cm), aggravated compressive deformation

Prevent collapse under major earthquakes	Severe damage stage	Significant damage	0.6~0.8	Tenon withdrawal (1.5~2cm), further aggravated compressive deformation, partial longitudinal fiber fracture
	Critical failure stage	Near collapse	0.8~1.0	Extensive fiber fracture, tenon withdrawal >2cm, substantial loss of load-bearing capacity

3.1.2 Joint reinforcement methods

3.1.2.1. Current research at home

Steel component reinforcement

Huan Junhong et al. (2019) [3] developed four flat steel reinforcement configurations for pre-damaged straight-tenon, penetrating-tenon, and dovetail joints, prioritizing the preservation of semi-rigid characteristics. Quasi-static cyclic tests systematically compared seismic performance parameters—including failure modes, hysteresis behavior, envelope curves, stiffness degradation, and energy dissipation capacity—before and after reinforcement. The research subjects and test specimens are shown in Figure 1.

Test piece number			Reinforcement	Is there	Screw or not
Half tenon	Through tenon	Dovetail joint	Device	Movable slot	Nail fixing
B0	T0	Y0			
B1	T1	Y1	1	Yes	No
B2	T2	Y2	2	No	No
B3	T3	Y3	3	Yes	Yes
B4	T4	Y4	4	No	Yes

Note: BO ~ B4,TO ~ T4,YO ~ Y4 in the table are the number of the test piece

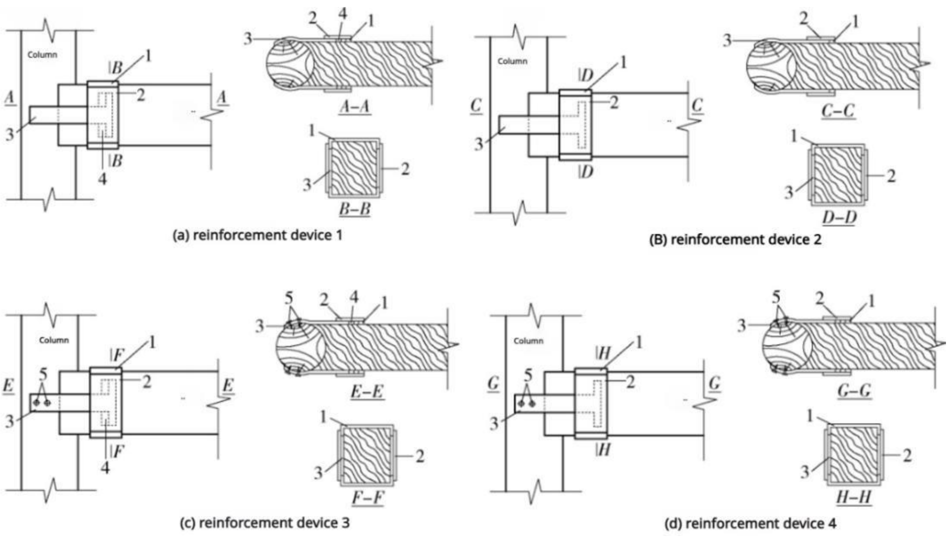

Figure 1. Steel component reinforcement device (Huan Junhong et al.,2019) [4]

Results [3] demonstrate that all reinforcement schemes enhance joint seismic performance, with screw-anchored column hoop systems (Devices 3 & 4) exhibiting the most significant improvement. By optimizing load-transfer efficiency at steel-timber interfaces, these systems achieve synergistic enhancement in peak load capacity, stiffness, and energy dissipation.

Sun Zhaoyang, Cheng Xiaowu, and Lu Weidong (2018)[5] reinforced straight-tenon joints with four distinct damage grades using embedded steel plates with self-tapping screws. Quasi-static loading tests captured hysteresis behavior, envelope curves, stiffness degradation patterns, and energy dissipation capacity. The research subjects and test specimens are shown in Figure 2.

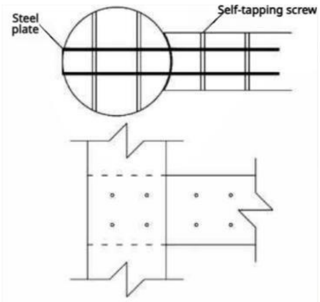

No	Damage type	Damage degree/%	Damaged volume/mm^3	Hole diameter/mm
W-0	None	0	0	0
C-1	Damage	7	119 000	5
C-2		15	178 500	6
C-3		25	297 500	6
GC-1	Damage (reinforcement)	7	119 000	5
GC-3		25	297 500	6

Figure 2. Reinforcement device of steel plates with self-tapping screws (Sun Zhaoyang, Cheng Xiaowu, and Lu Weidong, 2018) [6]

Results [5] indicate that this reinforcement significantly enhances joint strength and stiffness but amplifies seismic demand while reducing energy dissipation capacity compared to unreinforced joints. Consequently, the embedded steel plate-screw system is recommended for structures with severe damage and significant strength/stiffness deficiencies.

Sparrow-brace dampers for joint reinforcement

Chen Qingjun et al. (2023) [7] proposed and fabricated sparrow-brace dampers for mortise-tenon joint reinforcement. Quasi-static cyclic tests compared two typical Cantonese ancestral hall frames with tenon-head joints before and after reinforcement, evaluating hysteresis loops, envelope curves, strength degradation coefficients, stiffness evolution, and energy dissipation capacity. The research subjects and test specimens are shown in Figure 3.

Test piece number	Beam height/mm	Beam Tenon width/mm	Beam clear span/mm	Column height/mm	Column diameter/mm		Node form		Damper
					Left	Right	Left	Right	
S1	100	55	820	1 750	117	150	Hoop tenon	Straight tenon	None
JGS1	100	55	820	1 750	117	150	Hoop tenon	Straight tenon	Yes
S2	130	60	1 759	2 210	150	150	Hoop tenon	Hoop tenon	None
JGS2	130	60	1 759	2 210	150	150	Hoop tenon	Hoop tenon	Yes

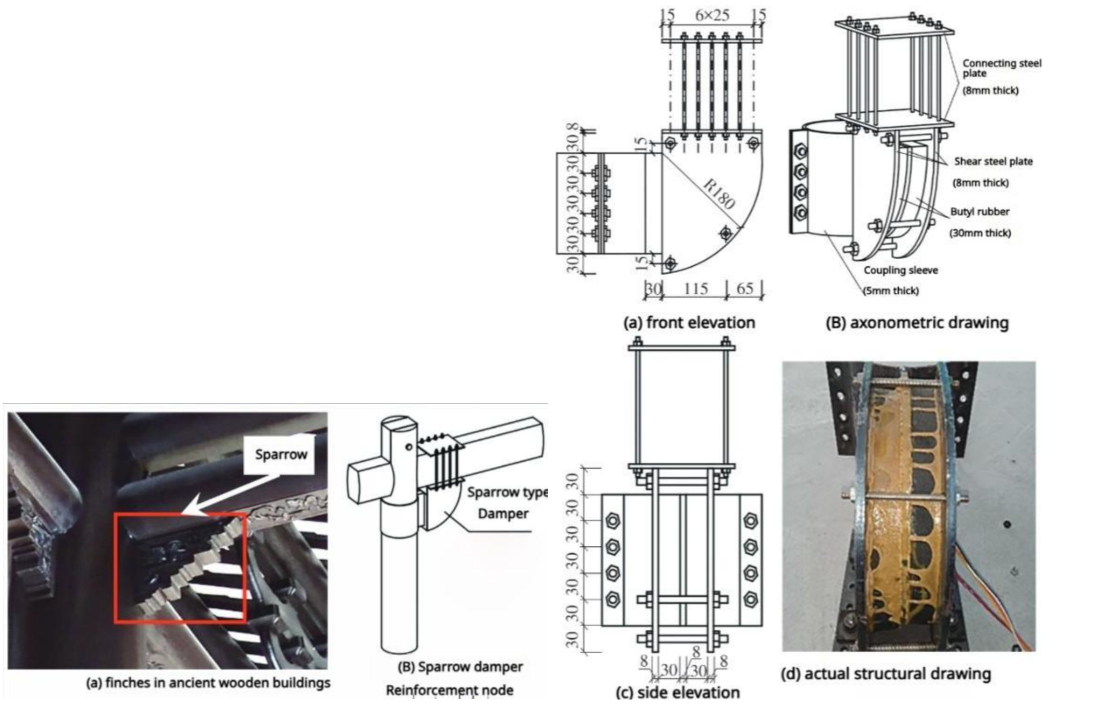

Figure 3. Test subjects and devices of sparrow-brace dampers reinforcement (Chen Qingjun et al., 2023) [8]

Results [7] demonstrate that the dampers effectively compensate for initial pre-loading damage by providing 45-68% higher initial stiffness at small rotations. As joints close at moderate rotations, the dampers engage in load-sharing synergy, enhancing ultimate load capacity, stiffness, and energy dissipation compared to unreinforced specimens.

Steel section-GFRP sheet composite reinforcement

Chu Yunpeng et al. (2024) [9] applied steel section-GFRP sheet composites to reinforce joints with varying loosening levels. Low-cycle tests compared seismic performance of originally loosened, strengthened, and post-earthquake retrofitted joints, comprehensively analyzing hysteresis behavior, envelope curves, stiffness evolution, energy dissipation, and tenon withdrawal-loosening correlation. The research subjects and test specimens are shown in Figure 4.

Group	Test piece No	Tenon length cut back Reduction/mm	tenon head length/mm	Loose momentum/ Tenon length	Group Description
Z1	DJ1	0	50	—	Loose Node
	DJ2	5	45	10%	
	DJ3	10	40	20%	
	DJ4	15	35	30%	
Z2	DG1	0	50	—	Reinforcement Node
	DG2	5	45	10%	
	DG3	10	40	20%	
	DG4	15	35	30%	
Z3	DC1	0	50	—	Solid Damage Node
	DC2	5	45	10%	
	DC3	10	40	20%	
	DC4	15	35	30%	

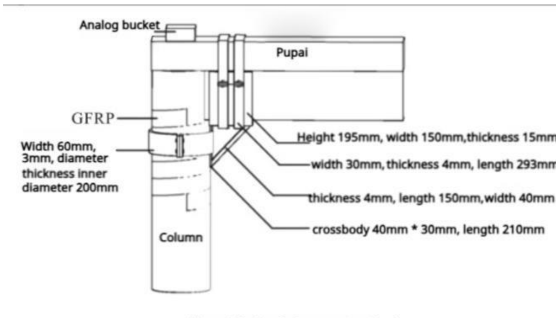

Figure 4. Test subjects and devices of Steel section-GFRP sheet composite reinforcement (Chu Yunpeng et al., 2024) [10]

Results [9] demonstrate that reinforcement effectively suppresses tenon disengagement, with strengthened joints exhibiting superior

Carbon fiber reinforced polymer reinforcement.

Xue Jianyang et al. (2012) [11] reinforced a damaged single-bay hall-style timber frame with carbon fiber reinforced polymer (CFRP) sheets. Three seismic waves were selected to investigate the dynamic responses of the reinforced model, including quantitative analyses of displacement, acceleration, seismic shear forces at column bases, column capitals, puzuo bracket sets, and rufu beams, as well as internal forces in mortise-tenon joints. Qualitative evaluations were performed on structural failure modes, dynamic characteristics, and torsional effects.The structure of the specimen is shown in Figure 5.

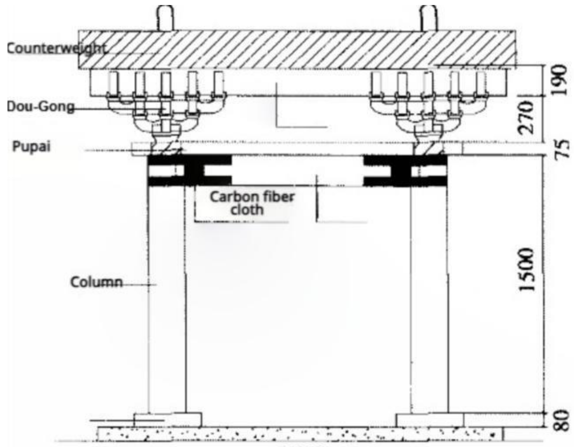

Figure 5. Plane graph of model (Xue Jianyang et al., 2012) [12]

Results [11] reveal that the seismic responses of the reinforced structure were significantly reduced through three energy-dissipation mechanisms: frictional slippage at column bases, rotation of semi-rigid mortise-tenon joints, and sliding within the dougong-puzuo bracket layers.

Wood wedge reinforcement

He Junxiao et al. (2022) [13] examined the impact of wood wedge reinforcement on the cyclic behavior of gap-existing penetrating tenon joints. Full-scale laboratory tests compared three joint models—intact joints, loosened joints, and wedge-reinforced joints—analyzing deformation patterns, failure modes, moment-rotation hysteresis, stiffness evolution, energy dissipation, and stress distribution. The research subjects and test specimens are shown in Figure 6.

Component name	Component size	Song feet	Model size/mm
Column	Diameter	36	390
	Column height	255	1 750
square column	Section height H	30	320
	Section width B	20	210
	Total length	250	2 625
Intact node (SJ)	Section width B		95
	Big Head length l2	18	195
	Large Head section height H	30	320
	Small head length	25	270
	Small Head section height h1	15	160
Loose node (LJ)	Large Head section height H		310
	Tenon joint gap Δ_g		10
Wooden Wedge reinforcement Node (WJ)	Large Head section height H		310
Wooden Wedge size	Long a		40
	Width c		20
	High B		95

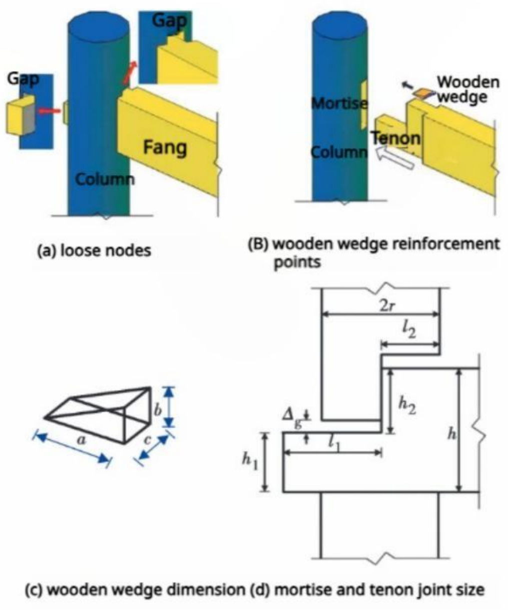

Figure 6. Test subjects and devices of wood wedge reinforcement (He Junxiao et al., 2022) [14]

Results [13] indicate intact and loosened joints exhibit longitudinal tearing failure propagating from the tenon neck to root, while reinforced joints develop wedge crushing failure. Wedge reinforcement substantially reduces joint slippage and pinching effects. Compared to degraded loosened joints, reinforced joints demonstrate approximately 30% higher bending capacity and restored energy dissipation performance.

3.1.2.2. Current research abroad

Carbon fiber reinforced polymer strips reinforcement

Minel Ahu Kara Alaşalvar et al. (2025) [15] reinforced timber beams sourced from three long-service structures with carbon fiber reinforced polymer (CFRP) strips. Three-point bending tests evaluated maximum load capacity, displacement at peak load, energy dissipation capability, and initial stiffness. Data acquisition integrated photographic documentation with digital image correlation (DIC) analysis and elastic curve diagrams. The structure of the specimen is shown in Figure 7.

Properties of the CFRP	Value	Picture
Specific Weight (g/m^2)	300 ± 10	
Thickness (mm)	0,12	
Tensile Strength (MPa)	4100	
Modulus of Elasticity (MPa)	231000	
Maximum Tensile Strain (%)	%1,7	

Figure 7. Mechanical and installation of properties of the CFRP (Minel Ahu Kara Alaşalvar et al., 2025) [16]

Comparative assessment of experimental results [15], DIC outputs, and elastic curve data against numerical models yielded the following conclusions: CFRP spaced at 50mm simultaneously optimized structural load capacity, initial stiffness, and deformation capability, demonstrating that closely spaced CFRP effectively constrains wood deformation to enhance global rigidity. CFRP spaced at 75mm achieved superior energy dissipation, indicating that moderately spaced strips permit controlled plastic deformation of wood for increased energy absorption. DIC analysis revealed post-reinforcement strain concentration at loading points and tensile zones (away from supports), confirming CFRP delays wood cracking by sharing tensile stresses and promotes uniform energy dissipation.

Timber pegs reinforcement

Carla Ceraldi et al. (2022) [17] evaluated the viability of reinforcing stop-splayed scarf joints with transverse keys using timber pegs as an all-wood solution. Monotonic axial tensile tests compared unreinforced joints with those reinforced by timber pegs, focusing on peg reinforcement efficacy. Key parameters investigated included load-bearing capacity, ductility, and the influence of slenderness ratio on joint behavior. The structure of the specimen is shown in Figure 8.

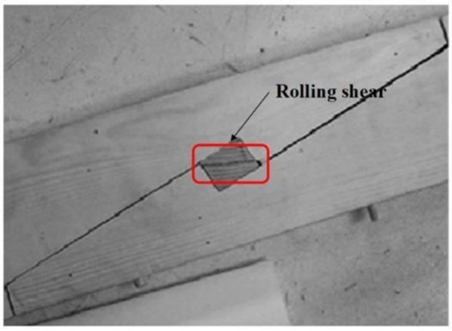

Figure 8. Timber pegs (Carla Ceraldi et al., 2022) [18]

Results [17] demonstrated that timber pegs significantly enhance joint performance by altering force-displacement constitutive behavior and force transfer mechanisms among connection components (transverse keys and timber boards) and delaying brittle failure modes seen in unreinforced specimens. Timber pegs exhibited 'effective peg shear' behavior—

characterized by peg flexure, shear deformation, and timber embedding—which preceded and mitigated brittle shear collapse in the heel region. This mechanism increased load capacity and ductility relative to unreinforced joints. Comparisons with prior tests on smaller joints (8mm-diameter pegs) revealed that higher slenderness ratios improve connection robustness (load capacity and ductility). For fixed board thickness, smaller-diameter pegs are preferable for joint reinforcement.

Self-tapping screws /Adhesive layer strengthening

Tannert and Thomas (2016) [19] experimentally investigated four methods to enhance the stiffness of Rounded Dovetail Joints (RDJs): (1) oversizing the dovetail section for tighter fit; (2) reinforcement with self-tapping screws; (3) adhesive layer strengthening; and (4) hybrid application of adhesive and screws. Testing recorded joint capacity at failure, deformation at collapse, and joint stiffness. The structure of the specimen is shown in Figure 9.

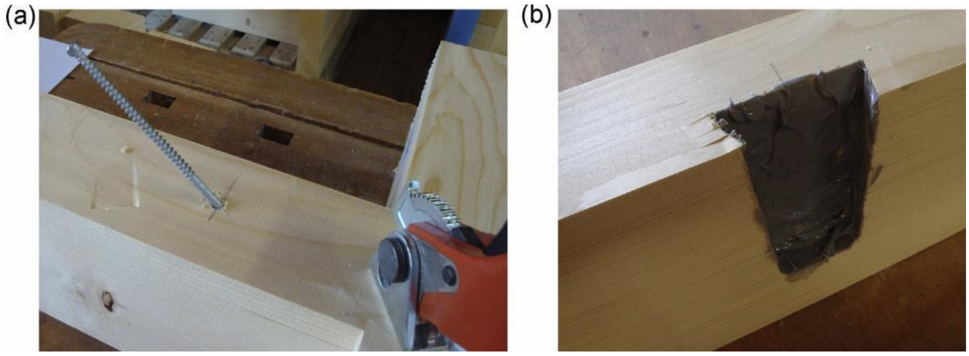

Figure 9. Detail showing reinforced RDJ: (a) use of STS; (b) use of adhesive layer. (Tannert and Thomas, 2016) [20]

Results [19] indicated that all methods significantly increased RDJ stiffness, yet this stiffness improvement incurred substantial reduction in deformation capacity. The hybrid method (screws plus adhesive) did not yield additional stiffness gain compared to adhesive-only reinforcement, suggesting screws function as a backup system to the adhesive layer in such composite joints.

3.2 Energy dissipation

3.2.1 Current research at home

Displacement-amplified rotational friction damper

Zhang Xicheng et al. (2022) [23] proposed and designed a displacement-amplified rotational friction damper. Quasi-static tests were conducted on straight-tenon joints before and after damper installation, with comparative analyses of failure modes, moment-rotation hysteresis relationships, skeleton curves, strength degradation patterns, stiffness degradation behaviors, and energy dissipation capacities. The displacement amplification effect and tenon withdrawal suppression capability of the damper were specifically investigated. The structure of the specimen is shown in Figure 10.

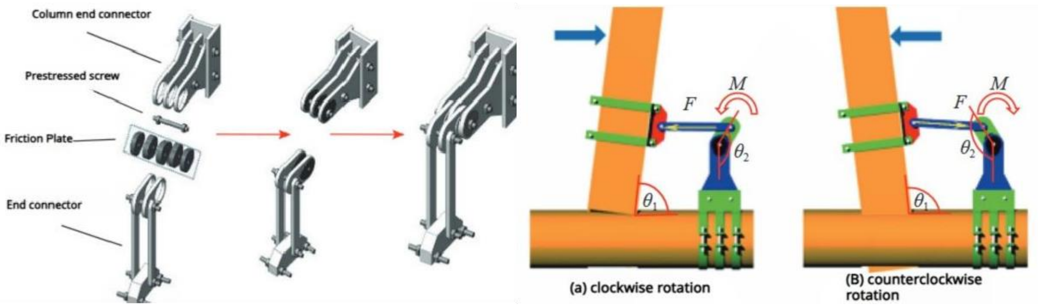

Figure 10. The device and action principle of displacement-amplified rotational friction damper (Zhang Xicheng et al., 2022) [22]

Results[23] indicate that: (1) The bending capacity of joints equipped with the damper increased by up to 230% compared to unreinforced joints; (2) The damper exhibits significant displacement amplification, achieving a maximum rotation angle 4.5 times greater than that of the mortise-tenon joint; (3) Without significantly increasing joint stiffness, the hysteretic energy dissipation capacity was substantially enhanced (up to 390%), with improvement magnitude positively correlated to bolt pretension strain; (4) The developed damper effectively suppresses tenon withdrawal, and this suppression effect intensifies significantly with increased bolt pretension strain.

Shape memory alloy (SMA) wires damping device

Zhang Xicheng et al. (2022) [23] developed a novel preventive reinforcement device using shape memory alloy (SMA) wires. Low-cycle reversed loading tests were conducted on five SMA-reinforced straight-tenon joints and one unreinforced control joint. The study systematically characterized failure modes, moment-rotation hysteresis relationships, strength/stiffness degradation patterns, energy dissipation capacity, self-centering capability, and deformation performance under varying SMA wire quantities and pre-strain levels, with a proposed analytical model for bending capacity calculation. The research subjects and test specimens are shown in Figure 11.

Test piece number	SMA wire			
	Diameter/mm	Root number	Pre-tensile strain/(%)	Length/mm
STJ-1	Unreinforced			
STJ-2	1.5	12	3	1500
STJ-3		16	3	
STJ-4		20	0	
STJ-5		20	1	
STJ-6		20	3	

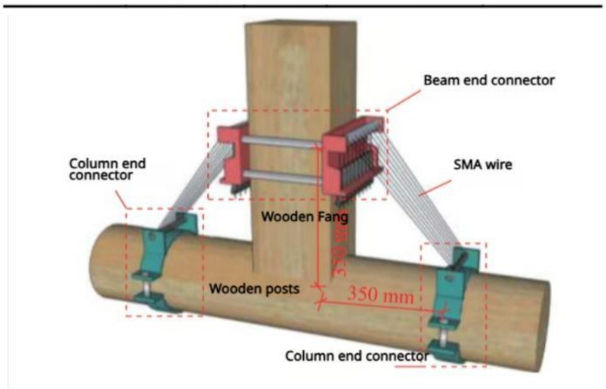

Fig. 2 Sketch of reinforced joint

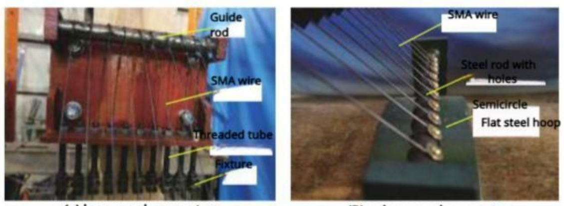

(a) beam end connector (B) column end connector

Figure 11. Test subjects and SMA wires damping device (Zhang Xicheng et al., 2022) [24]

Results[23] demonstrate49% increase in bending capacity and 124% higher maximum rotational stiffness compared to unreinforced joints; 37% reduction in strength degradation rate, confirming SMA's sustained resistance at large rotations (>0.05 rad); Energy dissipation capacity peaks at 0.03-0.04 rad before declining, contrasting with monotonic decrease in unreinforced joints; 60% less residual deformation and 2.3× enhanced self-centering efficiency with increased SMA wires/pre-strain

Fan-shaped viscoelastic dampers

Gao Yonglin et al. (2017) [25] installed fan-shaped viscoelastic dampers at the mortise-tenon joints of a timber structural model. Comparative shaking table tests were conducted on models with and without fan-shaped viscoelastic dampers. The test specimens are shown in Figure 12.

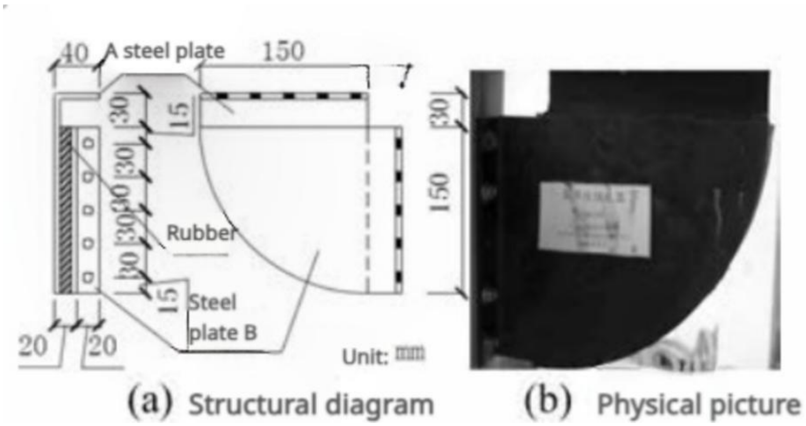

Figure 12. Constructing graphs and plane graphs (Gao Yonglin et al., 2017) [26]

Results [25] demonstrate that installing fan-shaped viscoelastic dampers at the joints significantly enhances tenon withdrawal resistance and improves the self-centering capacity of the structure, thereby meeting the seismic design requirements specified in the Chinese Code for Seismic Design of Buildings.

3.2.2 Current research at aboard

Connecting-type Visco-elastic Damper

SUZUKI et al. (2001) [27] designed a viscoelastic damper consisting of three triangular stainless-steel plates, with two layers of viscoelastic material inserted between each pair of plates. One of the steel plates is rigidly connected to the column, while the other is tightly fixed to the tie beam. The viscoelastic material deforms in response to rotational displacement of the connectors, thereby achieving energy dissipation. The test specimens are shown in Figure 13.

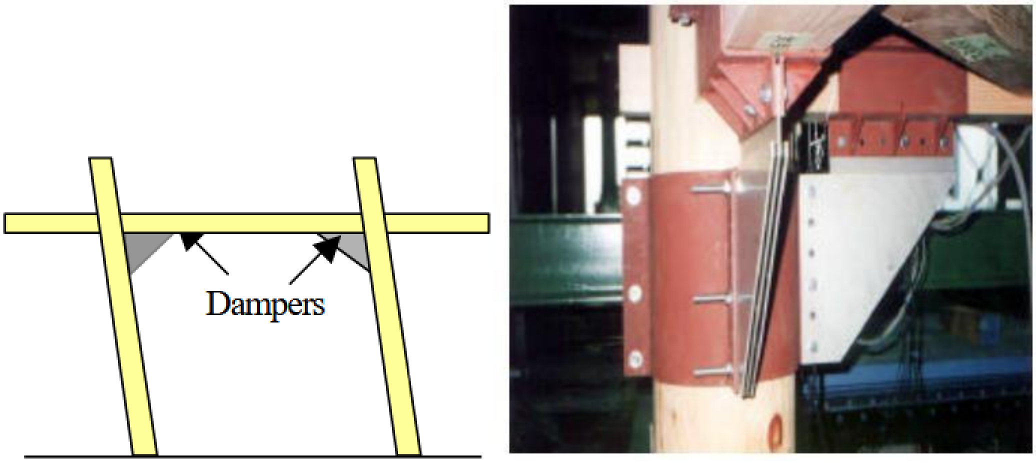

Figure 13. Installation of connecting-type dampers (SUZUKI et al., 2001) [28]

Through a series of shaking table tests [27], it was found that the connection-type viscoelastic damper effectively improves the seismic performance of traditional timber buildings. Specifically, the installation of such dampers increases the damping force of the timber structure and enhances the connectivity of the wooden frame. Additionally, this damper offers the advantage of straightforward installation.

Brake damper

SUZUKI et al. (2001) [27] designed a brake damper, a novel seismic damage control system. The damper primarily comprises high-tension bolts, stainless steel plates, brake pads, and conical disk springs. It is installed in various connections, such as beam-column joints and bracing connections. The structure of the device is shown in Figure 14.

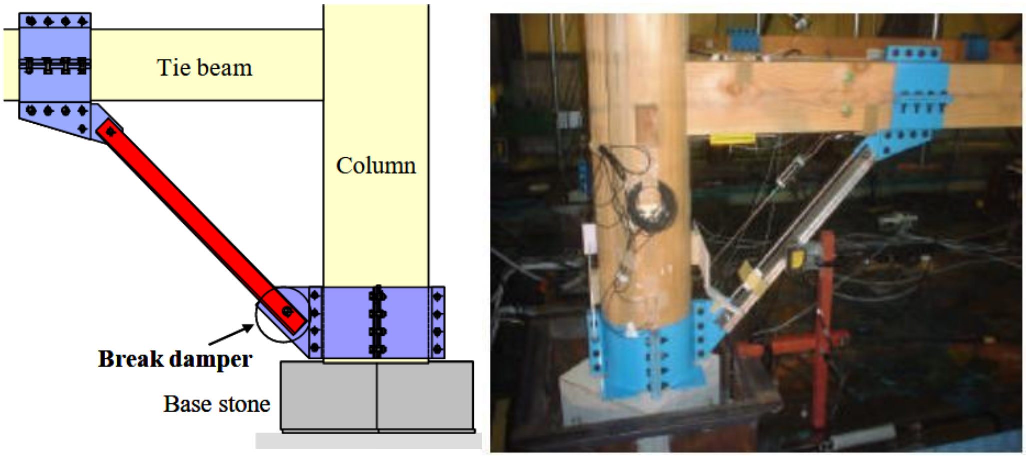

Figure 14. Installation of brake damper (SUZUKI et al., 2001) [29]

Shaking table test results [27] demonstrate that the brake damper provides stable restoring force characteristics and enhances damping capacity. During strong winds or earthquakes, these dampers initiate smooth sliding and utilize frictional damping to absorb seismic energy. The system exhibits structural simplicity, requiring no component replacement or specialized maintenance.

Wall damper

SUZUKI et al. (2001) [27] designed a wall damper primarily composed of a sealed container, an inner steel plate, silicone oil, and a cover plate. During shaking table tests, two dampers were installed between the foundation and the waist tie beam: the container was fixed to the shaking table, while the inner plate was rigidly connected to the waist tie beam. The test specimens are shown in Figure 15.

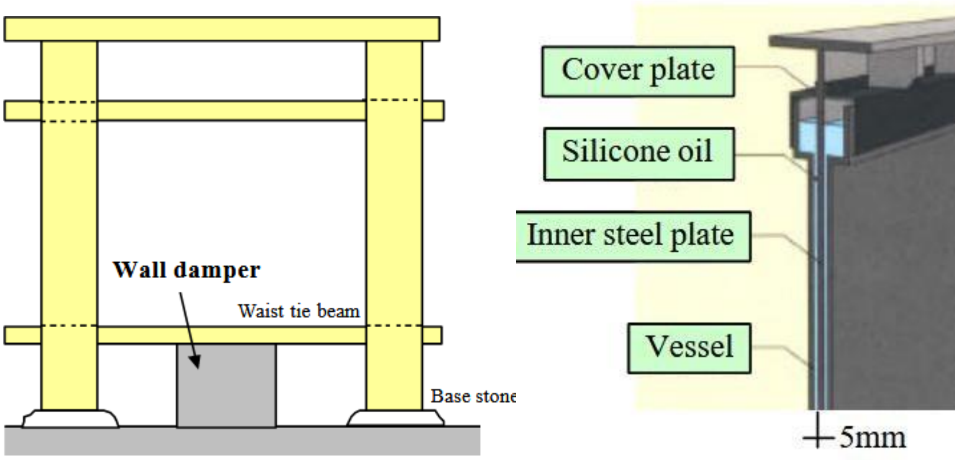

Figure 15. Installation of wall dampers (SUZUKI et al., 2001) [30]

Results [27] indicate that installing the wall damper significantly enhances energy dissipation capacity, whereas the overall structural stiffness remains virtually unchanged. The wall damper effectively increases damping capacity without altering structural stiffness.

Isolation system

WATABE et al. (2012) [31] implemented an isolation system utilizing custom resin-PTFE steel sliding bearings for horizontal isolation. Large H-shaped steel frames clamped the timber column bases from all sides, rigidly connecting them to the isolation system while incorporating superstructure reinforcement. The test specimens are shown in Figure 16.

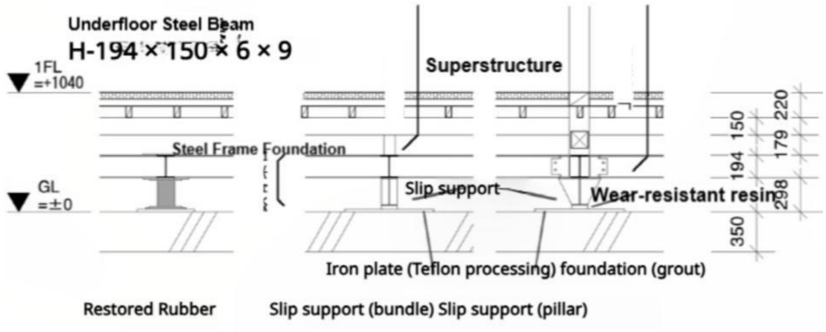

Figure 16. Isolation system (WATABE et al., 2012) [32]

Precision numerical simulations and ultimate load-bearing capacity calculations [31] revealed that the response acceleration of the isolated structure decreased substantially, and the actual response displacement was significantly lower than analytical predictions neglecting the fixed-base effect at column feet. Future work requires empirical validation of these effects and rigorous investigation into the consistency between models and physical responses.

MOCHIZUKI et al. (2017) [33] installed an isolation system beneath the stone platforms (kidan) of the Main Hall (Honden) and Provisional Hall (Gonden) at Kenkuni Shrine. The isolation layer, constructed with reinforced concrete, utilizes high-durability concrete and epoxy-coated steel bars to achieve a lifespan equivalent to the centuries-old timber structure. The isolation devices comprise low-horizontal-stiffness ball bearings and oil dampers. The foundation was treated with deep mixing improvement technology, forming a lattice-shaped reinforcement body surrounding the subsoil to prevent liquefaction during earthquakes. Structural responses (displacement and acceleration) were tested under extremely rare seismic events. The structure of the device is shown in Figure 17.

Figure 17. Isolation layer (MOCHIZUKI et al., 2017) [34]

Results [33] demonstrate that isolation reduced timber structure displacement responses to less than 1/50 and acceleration responses to below 1/4 compared to non-isolated counterparts. This technique eliminates the need for additional reinforcement beyond embedded wall panels, thereby enhancing seismic performance while preserving column aesthetics.

Zinc-Aluminum dampers

MOCHIZUKI et al. (2017) [33] implemented zinc-aluminum dampers at column-bracket connections of the triple-tiered pagoda in Hotel Chinzanso Tokyo. These dampers, fabricated from superplastic Zn-Al alloy and geometrically optimized for effective energy dissipation in column-bracket joints, underwent seismic simulations and static incremental analysis under extremely rare wind loads. The test specimens are shown in Figure 18.

Figure 18. Zinc-Aluminum dampers (MOCHIZUKI et al., 2017) [35]

Results [33] confirm that the isolation system meets predefined performance criteria, with Zn-Al dampers significantly reducing seismic deformation.

3.3 Column Base reinforcement

Column base hooping

Suda et al. (2012) [36] proposed a seismic retrofitting method for traditional timber structures by enlarging the column base cross-section to enhance restoring force characteristics induced by column rocking. Full-scale static lateral loading tests on traditional timber frames from Kyoto temples were conducted to analyze seismic reinforcement effects and validate design specifications of base-strengthening components. The structure of the device is shown in Figure 19.

Figure 19. Reinforcement members and Situation of reinforced column bottom (Suda et al., 2012) [37]

Results [36] demonstrated that: The method significantly improved column rocking restoring forces, particularly under large deformations; Reinforced frames exhibited superior deformation capacity and restoring force performance. This technique is applicable for seismic retrofitting of historic timber structures with large-diameter columns.

Orthogonal nagashi reinforcement

MOCHIZUKI et al. (2017) [33] developed an orthogonal nagashi reinforcement system to enhance the horizontal load-bearing capacity of foundation-level columns at Shonenji Temple. Nagashi members with identical section heights were orthogonally arranged above and below columns, interconnected via bolts and angle steels, while column-to-nagashi interfaces relied solely on surface contact without mechanical fasteners. Load capacity was calculated using existing bearing capacity formulas. The structure of the device is shown in Figure 20.

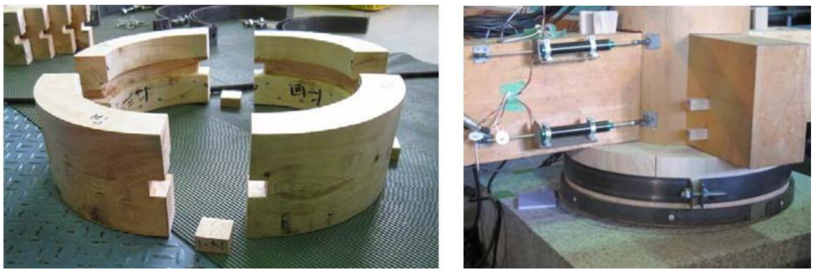

Figure 20. Reinforcement summary diagram (MOCHIZUKI et al., 2017) [38]

The results [33] demonstrated that applying this reinforcement to almost all columns significantly improved eccentricity, with deformation angles at various limit states reaching approximately 1/20. Furthermore, this method not only allows for reinforcement beneath the floor but also enables balanced reinforcement of all columns in both X and Y directions without positional bias, contributing effectively to eccentricity mitigation, that is, reducing the extent of column deviation from the base central axis during seismic activity. Additionally, by forming a U-shaped reinforcement around the columns, it prevents collapse caused by independent structural behavior of individual columns.

4. Conclusion and Prospect

1. Traditional timber structures inherently form a multi-layer isolation system through column base slippage, mortise-tenon joint rotation, dougong energy dissipation, and roof inertial effects. Seismic retrofitting must preserve these intrinsic mechanisms. Modern approaches prioritize two strategies: joint reinforcement and energy dissipation.

2. Joint reinforcement typically employs steel components, self-tapping screws (for joints with stiffness disparities), dampers, fiber materials (for slightly damaged joints), or wooden wedges (aesthetic preservation). While enhancing load-bearing capacity and stiffness, these methods generally increase global structural stiffness, consequently amplifying seismic forces. Crucially, neglecting internal force redistribution may cause adverse structural impacts when localized over-reinforcement occurs.

3. Energy dissipation techniques utilize friction dampers, shape-memory alloy dampers, viscoelastic dampers, and isolation systems. Subfloor reinforced concrete isolation layers partially maintain architectural authenticity.

4. Most methods compromise aesthetic integrity despite improving safety, violating the "authentic restoration" principle. The critical challenge remains developing bio-sourced or heritage-compatible devices to deliver sufficient damping while adhering to conservation ethics.

REFERENCES

[1] Wang, L., Zheng, J.G., Qian, C.Y. et al. (2024) ' Present situation and prospect on seismic and anti-vibration technology of ancient buildings', Journal of Natural Disasters, 33(02), pp. 1-17. DOI: 10.13577/j.jnd.2024.0201.
[2] Li, J.X., Bai, F.Y., Wang, Y.S. et al. (2024) ' Study on earthquake damage evolution model of through-mortise joints in ancient wooden structures', Building Structure, 54(12), pp. 146-152. DOI: 10.19701/j.jzjg.20212206.
[3] Huan, J.H., Ma, D.H., Guo, X.D. et al. (2019) ' Experimental Study of Aseismic Behaviors of Flexural Tenon Joint, Through Tenon Joint and Dovetail Joint Reinforced with Flat Steel Devices', Journal of Beijing University of Technology, 45(08), pp. 763-771. DOI:10.11936/bjutxb2018010012.
[4] Huan, J.H., Ma, D.H., Guo, X.D. et al. (2019) Figure 1. Steel component reinforcement device.
[5] Sun, Z.Y., Cheng, X.W. & Lu, W.D. (2018) 'Experimental study on seismic performance of damaged straight mortise-tenon joints of ancient timber buildings strengthened with steel plates and self-tapping screws', Structural Engineers, 34(05), pp. 106-112.
[6] Sun, Z.Y., Cheng, X.W. & Lu, W.D. (2018) Figure 2. Reinforcement device of steel plates with self-tapping screws.
[7] Chen, Q.J., Li, B.Z., Chen, Y.N. et al. (2023) ' Seismic Performance of Hoop Head Tenon Frame Structure Reinforced by Sparrow Brace Type Damper', Journal of South China University of Technology (Natural Science Edition), 51(04), pp. 9-20. DOI: 10.12141/j.issn.1000-565X.220160.
[8] Chen, Q.J., Li, B.Z., Chen, Y.N. et al. (2023) Figure 3. Test subjects and devices of sparrow-brace dampers reinforcement.
[9] Chu, Y.P., Fan, S.Q., Wang, S.Q. et al. (2024) ' Comparative test on seismic performance of dovetail joints of loose and strengthened wooden structures', Journal of Xi'an University of Architecture & Technology (Natural Science Edition), 56(05), pp. 679-689+700. DOI:10.15986/j.1006-7930.2024.05.006.
[10] Chu, Y.P., Fan, S.Q., Wang, S.Q. et al. (2024) Figure 4. Test subjects and devices of Steel section-GFRP sheet composite reinforcement.
[11] Xue, J.Y., Zhang, F.L., Zhao, H.T. et al. (2012) ' Shaking table test of an ancient timber structure strengthened with CFRP', China Civil Engineering Journal, 45(11), pp. 95-104.
[12] Xue, J.Y., Zhang, F.L., Zhao, H.T. et al. (2012) Figure 5. Plane graph of model.
[13] He, J.X., Wang, J., Yang, Q.S. et al. (2022) ' Effects of wedge strengthening on seismic performance of loose penetrated mortise-tenon joint', Journal of Civil and Environmental Engineering, 44(02), pp. 91-97. DOI: 10.11835/j.issn.2096-6717.2021.028.
[14] He, J.X., Wang, J., Yang, Q.S. et al. (2022) Figure 6. Test subjects and devices of wood wedge reinforcement.
[15] Kara Alaşalvar, M.A., Sağıroğlu Demirci, Ö., Tuna Akkaya, S., Türer, A., Çelik, A., Mercimek, Ö. & Anıl, Ö. (2025) 'Flexural behaviour of old wooden beams strengthened with CFRP: Experimental and numerical investigations' [Online]. Available at: https://www.sciencedirect.com/science/article/pii/S2352012425005326 (Accessed: 13 August 2025).
[16] Kara Alaşalvar, M.A., Sağıroğlu Demirci, Ö., Tuna Akkaya, S., Türer, A., Çelik, A., Mercimek, Ö. & Anıl, Ö.

(2025) Figure 7. Mechanical and installation of properties of the CFRP.
[17] Ceraldi, C., Sandoli, A., Lippiello, M. & Prota, A. (2021) 'Role of timber pegs in reinforcing stop-splayed scarf joints' [Online]. Available at: https://www.sciencedirect.com/science/article/pii/S2352710222007999 (Accessed: 14 August 2025).
[18] Ceraldi, C., Sandoli, A., Lippiello, M. & Prota, A. (2022) Figure 8. Timber pegs.
[19] Tannert, T. & Thomas, S. (2016) 'Improved performance of reinforced rounded dovetail joints' [Online]. Available at: https://linkinghub.elsevier.com/retrieve/pii/S0950061816307607 (Accessed: 15 August 2025).
[20] Tannert, T. & Thomas, S. (2016) Figure 9. Detail showing reinforced RDJ: (a) use of STS; (b) use of adhesive layer.
[21] Zhang, X.C., Han, Y.N., Qiu, Z.H. et al. (2022) ' EXPERIMENTAL STUDY ON SEISMIC PERFORMANCE OF MORTISETENON JOINTS STRENGTHENED WITH DISPLACEMENT-AMPLIFIED ROTATIONAL FRICTION DAMPER', Engineering Mechanics, 39(10), pp. 120-130. DOI: 10.6052/j.issn.1000-4750.2021.06.0434.
[22] Zhang, X.C., Han, Y.N., Qiu, Z.H. et al. (2022) Figure 10. The device and action principle of displacement-amplified rotational friction damper.
[23] Zhang, X.C., Hu, C.M., Wu, C.W. et al. (2022) ' RESEARCH ON ASEISMIC BEHAVIOR OF STRAIGHT TENON JOINTS REINFORCED BY SMA STRINGS IN ANCIENT TIMBER BUILDINGS', Engineering Mechanics, 39(04), pp. 164-176. DOI: 10.6052/j.issn.1000-4750.2021.02.0123.
[24] Zhang, X.C., Hu, C.M., Wu, C.W. et al. (2022) Figure 11. Test subjects and SMA wires damping device.
[25] Gao, Y.L., Tao, Z., Ye, L.Y. et al. (2017) ' Shaking table tests for a chuan-dou timber building with viscoelastic dampers', Journal of Vibration and Shock, 36(01), pp. 240-247+260. DOI: 10.13465/j.cnki.jvs.2017.01.035.
[26] Gao, Y.L., Tao, Z., Ye, L.Y. et al. (2017) Figure 12. Constructing graphs and plane graphs.
[27] Suzuki, Y., Katagihara, K., Iwasa, Y., Takata, K., Yamamoto, M., Goto, M. & Kitahara, A. (2001) 'Dynamic characteristics and seismic performance of traditional wooden structure by shaking table tests' [Online]. Available at: https://www.researchgate.net/publication/269661529_Dynamic_characteristics_and_seismic_performance_of_traditional_wooden_structure_by_shaking_table_tests (Accessed: 13 August 2025).
[28] Suzuki, Y., Katagihara, K., Iwasa, Y., Takata, K., Yamamoto, M., Goto, M. & Kitahara, A. (2001) Figure 13. Installation of connecting-type dampers.
[29] Suzuki, Y., Katagihara, K., Iwasa, Y., Takata, K., Yamamoto, M., Goto, M. & Kitahara, A. (2001) Figure 14. Installation of brake damper.
[30] Suzuki, Y., Katagihara, K., Iwasa, Y., Takata, K., Yamamoto, M., Goto, M. & Kitahara, A. (2001) Figure 15. Installation of wall damper.
[31] Watabe, M., Fujita, K. & Chiba, K. (2012) 'STRUCTURAL ANALYSIS OF A TIMBER MAIN HALL OF A TEMPLE BEFORE AND AFTER BASE-ISOLATED RETROFIT' [Online]. Available at: https://www.jstage.jst.go.jp/article/aijt/18/39/18_517/_article/-char/ja/ (Accessed: 13 August 2025).
[32] Watabe, M., Fujita, K. & Chiba, K. (2012) Figure 16. Isolation system.
[33] Mochizuki, E., Sugai, J. & Yamamoto, S. (2017) 'Seismic Reinforcement Techniques for Japanese Traditional Wooden Buildings' [Online]. Available at: https://www.jstage.jst.go.jp/article/jsms/66/11/66_829/_pdf/-char/en (Accessed: 14 August 2025).
[34] Mochizuki, E., Sugai, J. & Yamamoto, S. (2017) Figure 17. Isolation layer.
[35] Mochizuki, E., Sugai, J. & Yamamoto, S. (2017) Figure 18. Zinc-Aluminum dampers.
[36] Suda, T., Suzuki, Y., Mukaibo, K. & Tasiro, Y. (2012) 'Seismic Performance Evaluation of Temple Traditional Building Reinforced by Restoring Force due to Column Rocking' [Online]. Available at: https://www.iitk.ac.in/nicee/wcee/article/WCEE2012_2147.pdf (Accessed: 15 August 2025).
[37] Suda, T., Suzuki, Y., Mukaibo, K. & Tasiro, Y. (2012) Figure 19. Reinforcement members and Situation of reinforced column bottom.
[38] Mochizuki, E., Sugai, J. & Yamamoto, S. (2017) Figure 20. Reinforcement summary diagram.